JOURNAL OF THE AMERICAN CHEMICAL SOCIETY

Subscriber access provided by REGIS UNIV

Article

Evidence for Single Electron Shift in a Lewis Acid Base Reaction

Zhaowen Dong, Hanna H. Cramer, Marc Schmidtmann, Lucas A. Paul, Inke Siewert, and Thomas Müller

J. Am. Chem. Soc., **Just Accepted Manuscript** • DOI: 10.1021/jacs.8b09214 • Publication Date (Web): 15 Oct 2018

Downloaded from http://pubs.acs.org on October 17, 2018

Just Accepted

"Just Accepted" manuscripts have been peer-reviewed and accepted for publication. They are posted online prior to technical editing, formatting for publication and author proofing. The American Chemical Society provides "Just Accepted" as a service to the research community to expedite the dissemination of scientific material as soon as possible after acceptance. "Just Accepted" manuscripts appear in full in PDF format accompanied by an HTML abstract. "Just Accepted" manuscripts have been fully peer reviewed, but should not be considered the official version of record. They are citable by the Digital Object Identifier (DOI®). "Just Accepted" is an optional service offered to authors. Therefore, the "Just Accepted" Web site may not include all articles that will be published in the journal. After a manuscript is technically edited and formatted, it will be removed from the "Just Accepted" Web site and published as an ASAP article. Note that technical editing may introduce minor changes to the manuscript text and/or graphics which could affect content, and all legal disclaimers and ethical guidelines that apply to the journal pertain. ACS cannot be held responsible for errors or consequences arising from the use of information contained in these "Just Accepted" manuscripts.

ACS Publications

is published by the American Chemical Society. 1155 Sixteenth Street N.W., Washington, DC 20036

Published by American Chemical Society. Copyright © American Chemical Society. However, no copyright claim is made to original U.S. Government works, or works produced by employees of any Commonwealth realm Crown government in the course of their duties.

Evidence for Single Electron Shift in a Lewis Acid Base Reaction

Zhaowen Dong,[†] *Hanna H. Cramer,*[†] *Marc Schmidtmann,*[†] *Lucas A. Paul,*[‡] *Inke Siewert,*[‡] *Thomas Müller*[*,†]

[†]Institute of Chemistry, Carl von Ossietzky University of Oldenburg, Carl von Ossietzky-Str. 9-11, D-26129 Oldenburg, Federal Republic of Germany, European Union.

[‡]Institute of Inorganic Chemistry, Göttingen University, Tammannstr. 4, D-37077 Göttingen, Federal Republic of Germany, European Union.

ABSTRACT: The Lewis acid base reaction between a nucleophilic hafnocene based germylene and tris-pentafluorophenylborane ($B(C_6F_5)_3$) to give the conventional B – Ge bonded species in almost quantitative yields is reported. This reaction is surprisingly slow and during its course, radical intermediates are detected by EPR and UV-vis spectroscopy. This suggests that the reaction is initiated by a single electron transfer step. The hereby-involved germanium radical cation was independently synthesized by oxidation of the germylene by trityl cation or strong silyl-Lewis acids. A perfluorinated tetraarylborate salt of the radical cation was fully characterized including an XRD analysis. Its structural features and the results of DFT calculations indicate that the radical cation is a hafnium(III) centered radical that is formed by a redox induced electron transfer (RIET) from the ligand to the hafnium atom. This valence isomerization slows down the coupling of the radicals to form the polar Lewis acid base product. The implications of this observation is shortly discussed in the light of the recent finding that radical pairs are formed in frustrated Lewis pairs.

1. INTRODUCTION

The concept of Lewis acid base reactions is central to chemistry. In general, the reaction between an electron pair donor and an electron pair deficient acceptor results in the formation of a ylide with a formal two-electron two-center bond.[1] The conventional textbook electron pushing suggests the involvement of an electron pair in this process (Figure 1a). Thirty-seven years ago, Pross and Shaik recognized that the related S_N2 reactions can be understood in terms of single electron shift reactions, which accounts for the observation of products derived from both the typical concerted associative reaction pathway as well as from single electron transfer.[2] Using this concept, the relationship between reactants and product in a Lewis acid base reaction is a single electron shift from the lone pair of the Lewis base (LB) to the empty acceptor orbital of the Lewis acid (LA) and two spin-paired electrons are generated in close proximity to each other. Coupling of these two electrons into a single bond leads to formation of the polar product LA^--LB^+ (Figure 1b, 1c). The energy gain provided by this coupling after the single electron shift favours the polar product over the products of the single electron transfer (SET) reaction, where no coupling occurs. Any factor that operates as to hinder the coupling process will tend to favour the SET pathway over the polar one.[2b] The recently detected SET reactions in frustrated Lewis pairs in which the steric bulk of the reaction partners inhibits the coupling process nicely support this concept.[3] A similar dichotomy between concerted reaction pathway and SET reaction was recently suggested in Diels Alder reactions.[4]

In this contribution, we will describe the Lewis acid base reaction between $B(C_6F_5)_3$ (BCF), one of the most widely used Lewis acids[5] and a nucleophilic germylene **1**, recently synthesized in our laboratory.[6] A fast valence isomerization of the oxidized germylene prevents immediate coupling after the electron shift and allows for the experimental detection of the radical pair after SET.

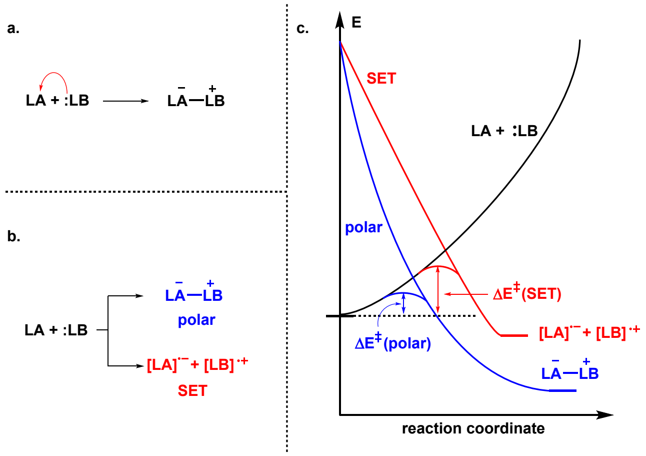

Figure 1. Lewis Acid (LA) / Base (LB) reaction. **a.** Textbook electron pushing description. **b.** Single electron shift which opens two pathways, the conventional polar (see a.) and the single electron transfer (SET) pathway. **c.** Schematic configuration mixing diagram for competing polar (blue) and SET (red) pathways.

2. RESULTS AND DISCUSSION

Syntheses. An equimolar ratio of a solution of BCF in toluene was added to a yellow toluene solution of the bicyclohexene-germylene (BCHGe) **1** at room temperature. After 12 h the color of the reaction mixture had changed from yellow to red-brown and the BCHGe/BCF Lewis adduct **2** was formed (Scheme 1a). It was isolated as red-brown oily product in nearly quantitative yield and was fully characterized by NMR-, UV-*vis* spectroscopy, and mass spectrometry. Orange crystals suitable for X-ray diffraction (XRD) analysis were obtained from toluene solution with slowly stirring the solution at room temperature. BCHGe/borane adduct **2** is stable at room temperature for more than half a year. The formation and stability of the Lewis adduct **2** in solution is shown by NMR spectroscopy. The chemical shifts of the ^{1}H NMR resonances of the two magnetically nonequivalent cyclopentadienyl (Cp) substituents (δ^{1}H = 5.00, 5.66) are clearly different from those of BCHGe **1** (δ^{1}H = 5.23, 5.55) but are similar to those of related BCHGe-Fe(CO)$_4$ (δ^{1}H = 5.05, 5.67) or BCHGe-W(CO)$_5$ (δ^{1}H = 5.08, 5.67) complexes[6a]. The relative sharp ^{11}B NMR resonance at δ^{11}B = 1.6 (half width w(1/2) = 600 Hz) indicate tetra-coordination for the boron atom in agreement with ^{19}F NMR data. In particular, the small NMR chemical shift difference between the signals for the *meta*- and *para*-fluorine atoms $\Delta\delta^{19}F_{m,p}$ ($\Delta\delta^{19}F_{m,p}$ = 8.5) is here informative.[7] In agreement with the NMR data, the solid state structure revealed the formation of the Lewis adduct **2** (Figure 2a). The structural parameter of the germylene unit of **2** are very close to that of the free BCHGe **1** (see Figure 2a and Table 1). In particular, the close approach of the germanium atom to the C^2=C^3 bond as shown by the small flap angle α(Ge) and the small Ge/C$^{2/3}$ separations indicate the stabilizing homoconjugative interaction.[6a, 8] The boron atom in compound **2** is tetra-coordinated and the Ge–B bond is relative long (226.0 pm) compared to standard values (Ge–B = 206 pm)[9] and to related complexes between germylenes and BCF (222.3 pm).[10] In qualitative agreement with the long Ge–B bond, its computed bond dissociation energy (BDE) is relatively small (BDE(B–Ge) (**2**) = 75 kJ mol^{-1}, at M06-2X/def2-tzvp). Compound **2** is a typical adduct between the Lewis basic BCHGe and Lewis acidic BCF.

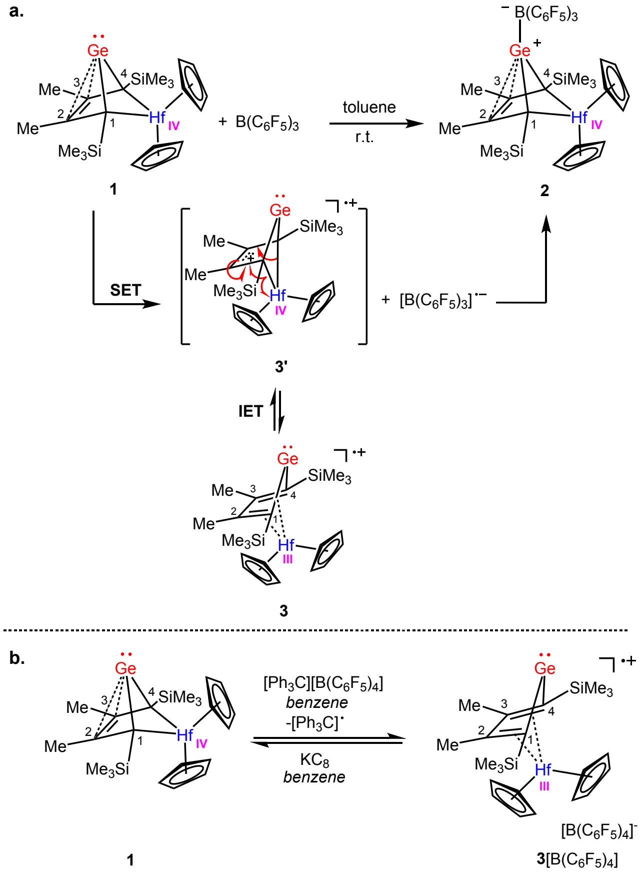

Scheme 1. The reactions of BCHGe 1 with diverse Lewis acids. a. Synthesis of the BCHGe/B(C$_6$F$_5$)$_3$ adduct **2** via radical complex **3**. **b.** The reaction of BCHGe **1** with [Ph$_3$C][B(C$_6$F$_5$)$_4$] to give the stable borate **3**[B(C$_6$F$_5$)$_4$] and the chemical reduction of radical cation **3** with KC$_8$ to recover BCHGe **1**.

Interestingly, in the course of 50 minutes after the addition of BCF, the toluene solution of BCHGe **1** turned to deep purple with a characteristic long wave absorption at λ_{max} = 544 nm. The intensity of this band decreases with time and after 6 h the typical red-brown solution of the BCF adduct **2** was obtained (λ_{max} = 394 nm, see Figures S2 – S4). The purple toluene solution was essentially NMR silent and electron paramagnetic resonance (EPR) investigations indicated the presence of two different radical species. One intensive, sharp signal (g_{iso} = 1.9881) with satellite signals due to hyperfine coupling to hafnium. The second broad resonance was partly obscured by the sharp signal (Figure S5). The intensity of the EPR signals decreased with time and essentially vanished after 3.5 h (Figure S6). A ^{1}H NMR spectra recorded after 6 h indicated the quantitative formation of the diamagnetic Lewis adduct **2**. We suggest that the intermediate radicals are formed in a single electron transfer process prior to the formation of the classical Lewis adduct (Scheme 1a).[11] The detection of hafnium satellites for the sharp EPR signal indicated that the radical [BCHGe]$^{\bullet+}$ **3** is derived from oxidation of BCHGe **1**. The resulting BCF radical anion, [BCF]$^{\bullet-}$, is the source for the UV-vis absorption at λ_{max} = 544 nm in toluene (r.t.) and of the broad, ill-defined EPR resonance. This is supported by the results of TD/DFT calculations that predict for [BCF]$^{\bullet-}$ an absorption at λ_{max} = 514 nm (Figure S30). [BCF]$^{\bullet-}$ has been characterized by the Norton group as a short living intermediate in THF ($t_{½}$ ≈ 2 min) and was suggested as reaction product resulting from reactions using BCF as oxidant.[11b] A deep blue color with λ_{max} ≈ 600 nm is reported for its solution in THF at T = -50

°C and the EPR spectrum consists of a 14-line signal centered at g_{iso} = 2.010.[11b, 12]

These observations suggest that the apparently simple Lewis acid / base reaction, shown in Scheme 1a, proceeds via a single electron transfer steps followed by coupling of the radical ions.

The cyclic voltammogram of BCHGe **1** showed an irreversible oxidation at E_{pa} = -0.51 V and a shoulder at –0.36 V in chlorobenzene (*vs.* $[Cp_2Fe]^+/[Cp_2Fe]$, ν = 0.1 Vs⁻¹, 0.1 M $[^nBu_4N][B(C_6F_5)_4]$, Figure S16). The shoulder vanishes at high scan rates, which points to a chemical reaction after initial oxidation forming a second redox-active product. Consistent with this, the peak potential shifts with increasing scan rates indicating fast chemical reaction after initial oxidation and/or irreversible electron transfer process (Figure S17).[13] Irrespectively of the scan rate, the shoulder is also present, when a mixture of **1** and BCF is measured, which indicates the formation of the same product after electrochemical oxidation and SET reaction of **1** and BCF (Figure S18). In line with the experimentally observed reversibility of reaction, the CV shows two reduction waves at –2.00 V and –2.27 V (*vs.* $[Cp_2Fe]^+/[Cp_2Fe]$, ν = 0.1 Vs⁻¹, Figure S19), which are only present after initial oxidation of **1**.

In order to gain more information about the intermediate radical cation **3** and to reach its fast quantitative formation, we switched to the stronger cationic oxidant trityl cation, $[Ph_3C]^+$ (*cf.* *E* = -0.11 V in MeCN[14]). As counter anion we choose the weakly coordinating $[B(C_6F_5)_4]^-$ anion, which provides additional kinetic stabilization of the radical cation due to its low reactivity. In addition, solutions of the salt $[Ph_3C][B(C_6F_5)_4]$ in aromatic hydrocarbons form biphasic mixtures of different polarity that allow separation of ionic from non-polar products.

After addition of 1 equiv. of $[Ph_3C][B(C_6F_5)_4]$ to a solution of BCHGe **1** in benzene, the color immediately changed from yellow to dark green. After 30 min reaction time, the two phases were allowed to separate and the upper non-polar light yellow benzene layer was investigated by EPR spectroscopy which indicated the presence of trityl radical ($Ph_3C^{\cdot}$) (Scheme 1b and S15). From the lower polar phase the residual solvent was removed and the deep-green oily residue was dissolved in chlorobenzene-d_5. As expected the sample was NMR silent but we detected the strong EPR signal of radical cation **3** (Figure 3) with clearly visible satellite signals due to hyperfine coupling to hafnium. Similar results were obtained when BCHGe **1** was treated with equimolar amounts of the silyl arenium borate $[Et_3Si(C_6H_6)][B(C_6F_5)_4]$ or with silylium borate $[(Me_5C_6)_3Si][B(C_6F_5)_4]$. In these cases no silyl centered radicals were detected, only secondary products such as $(Me_5C_6)_3SiH$ and $(Me_5C_6)_3SiMe$ were identified by NMR spectroscopy (see SI material).[15] Under these conditions radical cation **3** is stable for an extended period of time as the intensity of the EPR singlet decreased only slightly during 14 d (Figure S14). UV-vis spectroscopy in toluene showed two bands at λ = 350 and 430 nm and two additional weak absorptions at λ = 615 and 825 nm. Finally, radical cation borate **3**$[B(C_6F_5)_4]$ was characterized by the result of an XRD analysis (see below). The chemical oxidation is fully reversible as reduction of a freshly prepared solution of radical cation borate **3**$[B(C_6F_5)_4]$ by an equimolar amount of KC_8 in benzene-d_6 resulted in the quantitative back-formation of BCHGe **1** as shown by ^1H NMR spectroscopy (Scheme 1b, Figure S22).

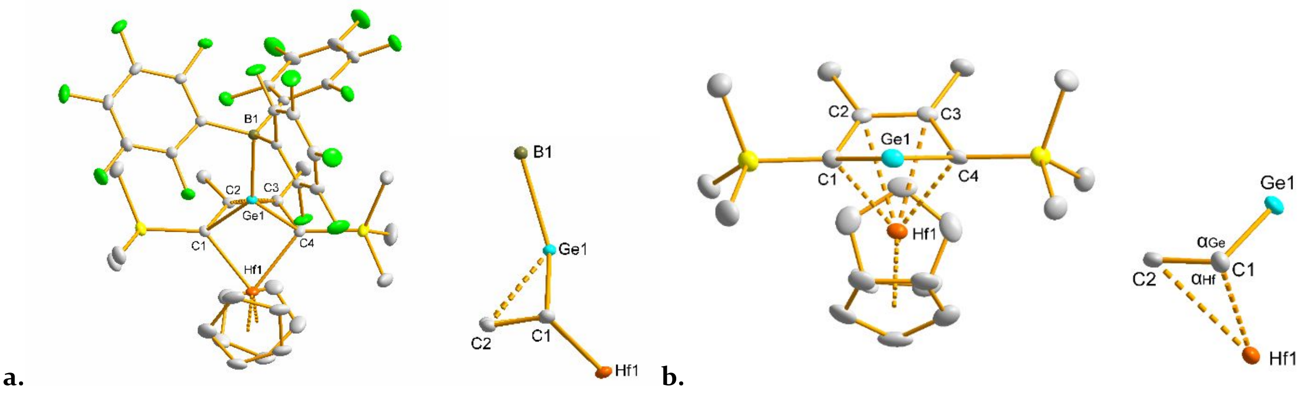

Figure 2. **a**. Molecular structure of Lewis adduct **2** in the (thermal ellipsoids at 50% probability, all hydrogen atoms are omitted for clarity). Selected atom distances [pm] and angles [°]: Ge1–B1 226.0(13), Ge1–C1 205.6(11), Ge1···C2 230.3(11), Ge1···C3 224.8(12), Ge1–C4 201.4(12), Ge1···Hf1 297.7(6), C1–C2 148.9(17), C2–C3 142.2(17), C3–C4 149.4(17), C1–Hf1 225.9(12), C2···Hf1 286.4(12), C3···Hf1 289.5(13), C4–Hf1 225.9(12), α(Ge) 100.5, α(Hf) 127.5. b. Molecular structure of radical cation **3** in the solid state. Thermal ellipsoids at 50% probability, all hydrogen atoms, solvent molecules and $[B(C_6F_5)_4]^-$ are omitted for clarity. Selected atom distances [pm] and angles [°], given as mean values from two independent molecules: Ge1–C1 203.1(4), Ge1···C2 260.7(36), Ge1···C3 262.4(37), Ge1–C4 203.5(4), Ge1···Hf1 289.9(6), C1–C2 142.6(5), C2–C3 144.7(5), C3–C4 142.9(5), C1–Hf1 233.4(4), C2–Hf1 269.5(37), C3–Hf1 268.5(36), C4–Hf1 232.0(3), α(Ge) 131.3, α(Hf) 110.1. For the definition of the flap angles, see Table 1.

Structural characterization of borate 3$[B(C_6F_5)_4]$. XRD analysis of yellow-green single crystals revealed two independent ion pairs of **3**$[B(C_6F_5)_4]$ in the asymmetric unit with well-separated radical cations **3** and borate anions (the shortest F / Hf or F / Ge atomic distances are 445.8 or 445.9 pm). The molecular structure of radical cation **3** differs significantly from that of BCHGe **1** and from the germylene fragment of the Lewis adduct **2**. (see Table 1, and Figure 2b). Common to all three molecular structures is the bent five-membered GeC_4 ring with a regular envelope conformation (Figure 2b, Table 1).[6a] The flap angle α(Ge) of 131.3° in cation **3** is however significantly larger than the flap angle α(Ge) of 97.9° in BCHGe **1**, which suggests that the homoconjugative interaction between the Ge atom and the remote C^2C^3 bond is canceled.[6b] This is further shown by larger atomic distances between the Ge and the $C^{2/3}$ atoms (260.7, 262.4 pm) compared with those in BCHGe **1** (226.7, 227.0 pm). The Ge–$C^{1/4}$ bond lengths of cation **3** (Ge–$C^{1/4}$ = 203.1, 203.5 pm) are typical for aryl- and alkyl-substituted germylenes (Ge–C = 200–209 pm).[16] The nearly equidistant inner cyclic C–C bonds of the GeC_4 ring (C–C = 142.6, 144.7, 142.9 pm) shows the delocalized structure of the butadiene fragment. The flap angle α(Hf) decreases significantly upon oxidation (**1**: α(Hf) = 124.8°; **3**: α(Hf) = 110.1°). This indicates the switch from the η^2-coordination of the hafnium atom to the C_4Ge ring in BCHGe **1** to the η^4 coordination in a σ^2, π-mode in cation **3**.[6b] In agreement, the Hf–$C^{1/4}$ bonds (Hf–$C^{1/4}$ = 233.4, 232.0 pm) and Hf–$C^{2/3}$ bonds (Hf–$C^{2/3}$ = 269.5, 268.5 ppm) in cation **3** all are longer than Hf–$C^{1/4}$ σ-bonds in BCHGe **1** (Hf–$C^{1/4}$ = 220.3, 220.1 pm)[6a] or the single bond covalent radii of Hf and C atoms (Hf–C = 227 pm).[9] The germanium and the hafnium atom in cation **3** are separated by 289.9 pm which falls out of the range of regular Hf – Ge single bonds (Ge–Hf = 273 pm)[9] and indicate only small bonding interaction between both centers. Summarized, these structural features indicate that cation **3** is best described as a η^4-butadiene hafnocene complex with an independent germylene functionality.

Table 1. Comparison of structural parameter of compounds 1-3 and calculated structure 2^{opt} and 3^{opt}.

	1[a]	**2**[b]	**2**^{opt}[c]	**3**[b]	**3**^{opt}[d]
C^1–C^2	148.3	148.9	148.9	142.6	141.6
C^2–C^3	142.5	142.2	142.0	144.7	145.3
C^3–C^4	148.2	149.4	149.1	142.9	141.2
C^1–Ge	210.0	205.6	202.8	203.1	203.2
C^2–Ge	226.7	230.3	223.6	260.7	262.3
C^3–Ge	227.0	224.8	220.8	262.4	261.3
C^4–Ge	208.8	201.4	203.8	203.5	203.4
B–Ge	–	226.0	224.9	–	–
C^1–Hf	220.3	225.9	225.0	233.4	235.0
C^2–Hf	277.9	286.4	281.8	269.5	267.8
C^3–Hf	278.5	289.5	284.5	268.5	268.0
C^4–Hf	220.1	225.9	224.3	232.0	235.8
Ge–Hf	301.0	297.7	302.7	289.9	295.2
C^4–Ge–C^1	85.0	86.6	86.6	85.7	85.5
α (Hf)[e]	124.8	127.5	124.8	110.1	107.5
α (Ge)[f]	97.9	100.5	97.2	131.3	132.4

[a] Experimental data from XRD, mean values from three independent molecules, reference 10. [b] Experimental data from XRD. [c] M06-2X/def2-tzvp. [d] UM06-2X/def2-tzvp. [e] Flap angle α(Hf) is defined as angle between the Hf atom, the midpoint of C^1/C^4 and midpoint of C^2/C^3 distances. [f] Flap angle α(Ge) is defined as angle between the Ge atom, the midpoint of C^1/C^4 and the midpoint of C^2/C^3 distances. [i] Sum of the covalent radii expected for Hf–E single bonds: E = C: 227 pm, E = Ge: 273 pm. Sum of the covalent radii expected for C–E single bonds: E = C: 150 pm, E = Ge: 196 pm.

EPR analysis and electronic structure of radical cation 3. Radical cation **3** was characterized by X-band EPR spectroscopy (Figure 3) at ambient temperature. The EPR spectrum in chlorobenzene showed an intense singlet accompanied by several satellite signals, which are characteristic for a hafnium-centered radical. This singlet showed the same spectroscopic characteristics as the hafnium centered radical species obtained from the reaction of BCF with germylene **1** (Figure S5). The experimental EPR spectrum of radical cation **3** was simulated based on the following parameter: g_{iso} = 1.9881, A_{iso}(Hf) = 8.5 mT (Figure 3). These EPR data indicated a localization of the unpaired electron at the hafnium atom. To gain further insight into the electronic structure of **3**, density functional calculations were performed for **3** at the UM06-2X/ADZP(Hf),def2-tzvppd(Ge,Si,C,H)//UM06-2X/def2-tzvp level. The calculated structure for radical cation **3** is very close to that determined by XRD analysis, the largest deviation in atomic distances being less than 2 % (Table 1). In agreement with the ESR spectroscopic results, the calculations indicated that the singly occupied molecular orbital (SOMO) and the total spin density distribution of **3** are mainly localised on the dz^2 orbital of the Hf atom with contributions from the π* orbital of the butadiene fragment and only minor contributions of the lone pair of the germanium atom (Figures 4a-4c). The highest doubly occupied molecular orbital is dominated by the lone pair at the germanium atom (Figure 4d) and the LUMO shows significant contributions from the 4p(Ge) orbital (Figure 4e). This arrangement of frontier orbitals point to the germylene nature of radical cation **3**. Time dependent (TD)-DFT calculations allowed the assignment of the long wave UV-absorption of radical cation **3** in toluene at λ_{max} = 825 nm to the SOMO → LUMO transition (calculated λ = 816 nm, Figure S29).

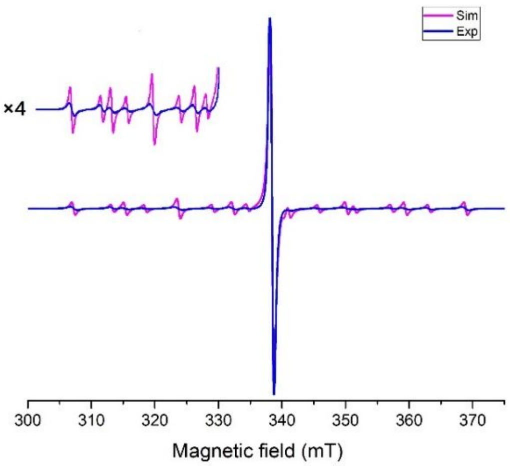

Figure 3. Experimental (blue solid lines) and simulated (pink solid lines) EPR spectrum for radical cation **3** in C_6H_5Cl solution was measured at 298 K (microwave frequency = 9.403 GHz). Fit parameters: g_{iso} = 1.9881, A_{iso}(Hf) = 8.5 mT. The simulated spectrum included an 18.6% ^{177}Hf contribution and 13.6% ^{179}Hf contribution.

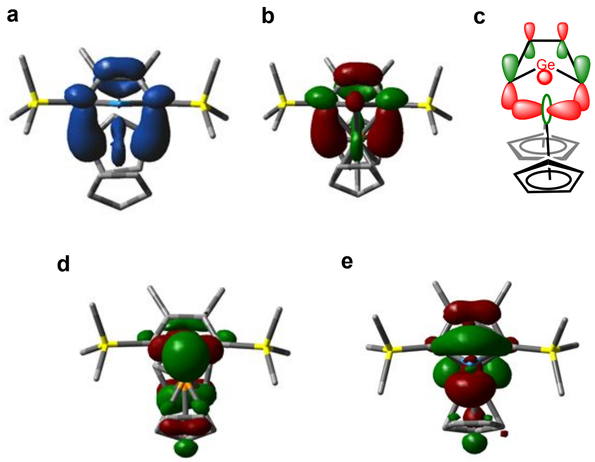

Figure 4. Spin density map and key frontier molecular orbitals of radical cation **3** calculated at the UM06-2X/ADZP(Hf), def2-tzvppd(Ge,Si,C,H) // UM06-2X/def2-tzvp level. a. Spin density map of 3^{opt} (isovalue = 0.004). b. Singly occupied molecular orbital (SOMO) of 3^{opt} (E = -9.07 eV). c. Sketch of the atomic orbital contributions of SOMO. d. Surface diagram of SOMO-1(α) of 3^{opt} (E = -10.88 eV). e. Surface diagram of LUMO(α) of 3^{opt} (E = -4.65 eV). (Color code: Yellow, silicon; blue, germanium; orange, hafnium; gray, carbon; all hydrogen atoms are omitted for clarity, isovalue for all MOs: 0.05).

Based on the computational investigations, EPR spectroscopy and XRD analysis, we conclude that radical cation **3** can be described as a hafnocene(III) complex which is η^4 coordinated in a σ^2, π-mode to a 1-germacyclopenta-2,4-dienylidene. Therefore, the oxidation of BCHGe **1** resulted in the formal reduction of the hafnium atom. As the HOMO of BCHGe **1** is a combination of the π-C^2C^3 orbital and the 4p(Ge) atom,[6a] the initial step of the one-electron oxidation is the formation of the alkene radical cation **3'** (Scheme 1). Cation radical **3'** undergoes a valence isomerization in the form of an intra-molecular electron transfer (IET) process, which changed the formal oxidation state of hafnium from +IV to +III. This process provides an additional example for a redox induced electron transfer (RIET) process,[17] in this involving the hafnium and a non-innocent butadiene ligand.

3. CONCLUSIONS

In conclusion, a new BCHGe/$B(C_6F_5)_3$ Lewis adduct **2** was obtained by the reaction of BCHGe **1** with $B(C_6F_5)_3$. This Lewis acid base reaction was surprisingly slow but proceeds with nearly quantitative yield. During this reaction the radical pair **3**[BCF] was identified by EPR and UV-vis spectroscopy. Using $[Ph_3C][B(C_6F_5)_4]$ or silylium borates as oxidants the radical cation **3** was selectively synthesized and isolated in the form of its tetraarylborate. Its formation is chemically reversible as its reduction with KC_8 gave quantitatively BCHGe **1**. Radical cation **3** is a hafnocene (III) complex, which is formed from the expected radical cation **3'** by an intramolecular electron transfer process from the ligand to the hafnium center. Scheme 1 summarizes these processes and suggests that this Lewis acid/base reaction proceeds via a SET reaction. The investigated example is unique as far as the described valence isomerization **3'** → **3** is fast and it hampers the formation of the Lewis adduct **2** as the electronic situation in **3** does not allow for an immediate coupling of the radical pair. Our results are in line with the idea that a Lewis acid base reaction proceeds via a single electron shift in the transition-state region and each factor that prevents coupling to the polar product favors the SET process.[2a] We are convinced that this work opens up new perspectives to Lewis acid / base chemistry, particularly in view of the recent discovery that frustrated Lewis pairs are prone to SET reactions.[3a, 3b]

4. EXPERIMENTAL SECTION

All the reactions were performed under dry argon atmosphere using standard Schlenk techniques or in a nitrogen-filled glovebox. BCHGe **1** was prepared according to a literature procedure.[6a] Non-chlorinated Solvents were dried over sodium/potassium alloy and distilled under nitrogen prior to use. Details of experimental procedures, EPR analytical data, UV-vis spectrum and X-ray structure determinations are given in the Supplementary Information. All quantum chemical calculations were carried out using the Gaussian09 package. The NBO analyses were performed with the Version 6.0 of the NBO program which was implemented in the G09 D.01 version of the Gaussian program.

Synthesis of germylene/borane adduct 2: A toluene (3 mL) solution of $B(C_6F_5)_3$ (84.48 mg, 0.165 mmol) was added to a yellow toluene solution (3 mL) of BCHGe **1** (100 mg, 0.165 mmol) at room temperature. The reaction mixture was stirred for overnight at room temperature. After that, the solvent was removed under vacuum and the red-brown oily residue was identified as germylenes/borane adduct **2** by NMR spectroscopy in almost quantitative yield.

Spectroscopic data of germylenes/borane adduct **2**: ^{1}H NMR (499.87 MHz, 305.0 K, C_6D_6): δ = 5.66 (s, 5H, Cp), 5.00 (s, 5H, Cp), 1.62 (s, 6H, 2xCH_3) 0.02 (s, 18H, $Si(CH_3)_3$). $^{13}C\{^1H\}$ NMR (125.71 MHz, 305.0 K, C_6D_6): δ = 148.1 (dm, *o*-$\underline{C}$F, $^1J(^{13}C\text{-}^{19}F)$ = 244 Hz), 141.3 (dm, *p*-$\underline{C}$F, $^1J(^{13}C\text{-}^{19}F)$ = 255 Hz), 137.7 (dm, *m*-$\underline{C}$F, $^1J(^{13}C\text{-}^{19}F)$ = 252 Hz), 136.4 (2x$\underline{C}CH_3$), 117.4 (br, *ipso*-$\underline{C}$), 104.5 (Cp), 103.4 (Cp), 103.2 (2x$\underline{C}$Si), 19.5 ($\underline{C}H_3$), 3.7 (2x$Si(\underline{C}H_3)_3$). $^{29}Si\{^1H\}$ NMR (99.31 MHz, 305.0 K, C_6D_6): δ = -3.4. $^{11}B\{^1H\}$ NMR (160.378 MHz, C_6D_6, 305 K): δ = 1.6. $^{19}F\{^1H\}$ NMR (470.348 MHz, C_6D_6, 305 K): δ = –162.5 (t, *m*-C$\underline{F}$, $^3J(^{19}F\text{-}^{19}F)$ = 20 Hz), –154.0 (tm, *p*-C$\underline{F}$, $^3J(^{19}F\text{-}^{19}F)$ = 17 Hz), –127.1 (dm, *o*-C$\underline{F}$, $^3J(^{19}F\text{-}^{19}F)$ = 19 Hz). HRMS (70 eV, CI) *m*/*z* $[M+H]^+$ Calcd for $C_{40}H_{35}BF_{15}GeHfSi_2$: 1121.0803 Found: 1121.0807. UV-vis (toluene solution) [nm]: λ = 294, 394(sh).

Synthesis of hafnium radical cation 3: A benzene (3 mL) solution of $[Ph_3C][B(C_6F_5)_4]$ (152.2 mg, 0.165 mmol) was slowly added to a yellow benzene solution (3 mL) of BCHGe **1** (100 mg, 0.165 mmol) at room temperature. Then the reaction mixture was stirred 30 min at this temperature and the solution turned from a yellow to a deep green biphasic mixture. After separation of the two phases, the upper benzene phase was investigated by EPR analysis and showed strong EPR signals, which suggested the formation of trityl radical. The lower layer was evaporated under vacuum and the residue was dissolved in C_6D_5Cl. The solution was NMR silent but showed an intensive EPR signal. Yellow-green single crystals suitable for X-ray diffraction analysis were obtained by recrystallization from toluene solution at 6 °C. (Yield: 167 mg (80%)).

ASSOCIATED CONTENT

Supporting Information. Experimental and computational details, NMR spectra and details of the structure solution of compounds **2**, **3** and $(Me_5C_6)_3SiMe$. This material is available free of charge via the Internet at http://pubs.acs.org.

AUTHOR INFORMATION

Corresponding Author

* thomas.mueller@uni-oldenburg.de

ORCID

Zhaowen Dong: 0000-0001-6163-470X

Thomas Müller: 0000-0002-4247-3776

Hanna H. Cramer: 0000-0001-7047-2511

Inke Siewert: 0000-0003-3121-3917

Lucas A. Paul: 0000-0001-9152-8668

Marc Schmidtmann: 0000-0001-8026-7271

Notes

The authors declare no competing financial interest.

ACKNOWLEDGMENT

This work was supported by the Carl von Ossietzky University Oldenburg, Göttingen University, by the Lower Saxony State (Lichtenberg Fellowship to Z.D.) and by the DFG (SI 1577/2-1). The simulations were performed at the HPC Cluster CARL, located at the University of Oldenburg (Germany) and funded by the DFG through its Major Research Instrumentation Program (INST 184/108-1 FUGG) and the Ministry of Science and Culture (MWK) of the Lower Saxony State.

REFERENCES

(1) (a) Jensen, W. B. *Chem. Rev.* **1978**, *78*, 1-22. (b) Denmark, S. E.; Beutner, G. L. Principles, Definitions, Terminology, and Orbital Analysis of Lewis Base–Lewis Acid Interactions Leading to Catalysis; In *Lewis Base Catalysis in Organic Synthesis*; Vedejs, E.; Denmark, S. E.; Eds.; Wiley-VCH, Weinhein: 2016, pp 31-54.

(2) (a) Shaik, S. S. *J. Am. Chem. Soc.* **1981,** *103*, 3692-3701. (b) Pross, A. *Acc. Chem. Res.* **1985,** *18*, 212-219. (c) Shaik, S. S. *Acta Chem. Scand.* **1990,** *44*, 205-221. (d) Eric, V.; Anslyn, D., *Modern Physical Organic Chemistry*. University Science Books: Sausalito, CA, 2006.

(3) (a) Liu, L. L.; Cao, L. L.; Shao, Y.; Ménard, G.; Stephan, D. W. *Chem* **2017,** *3*, 259-267. (b) Liu, L. L.; Cao, L. L.; Zhu, D.; Zhou, J.; Stephan, D. W. *Chem. Commun.* **2018,** 54, 7431-7434. (c) Piers, W. E.; Marwitz, A. J.; Mercier, L. G. *Inorg. Chem.* **2011,** 50, 12252-12262. (d) Merk, A.; Großekappenberg, H.; Schmidtmann, M.; Luecke, M.-P.; Lorent, C.; Driess, M.; Oestreich, M.; Klare, H.; Müller, T. *Angew. Chem. Int. Ed.*, in press, DOI: 10.1002/anie.201808922.

(4) Cahill, K. J.; Johnson, R. P. *J. Org. Chem.* **2012,** *78*, 1864-1873.

(5) Piers, W. E.; Chivers, T. *Chem. Soc. Rev.* **1997,** *26*, 345-354.

(6) (a) Dong, Z.; Reinhold, C. R. W.; Schmidtmann, M.; Müller, T. *Angew. Chem. Int. Ed.* **2016,** 55, 15899-15904. (b) Dong, Z.; Bedbur, K.; Schmidtmann, M.; Müller, T. *J. Am. Chem. Soc.* **2018,** *140*, 3052-3060.

(7) The ^{19}F NMR of BCF can offer a reliable probe of the coordination environment around the boron atom. The planar structure of BCF allows efficient resonance between the empty 2p-orbital at the boron atom and the π-system of the perfluorinated aryl-substituent. This π-resonance leads to significant deshielding of the *p*-fluorine atom. Coordination of a fourth substituent to the boron atom results in loss of planarity and hampers the resonance. As a consequence, the signal of the *p*-fluorine atom moves to higher field. The fluorine atoms in the *meta* positions are not influenced by the π-resonance and their ^{19}F NMR chemical shifts do not change significantly by pyramidalization of the boron center. Therefore, the separation between the *meta* and *para* ^{19}F chemical shifts ($\Delta\delta_{m,p}$) is a convenient measure for the pyramidalization of the boron atom. For neutral tri-coordinated BCF it is large ($\Delta\delta^{19}F_{m,p}$ (BCF) = 20.1), and it becomes smaller in neutral tetra-coordinated boron compounds and in anionic borates (i.e. $\Delta\delta^{19}F_{m,p}$ (**2**) = 8.5; $\Delta\delta^{19}F_{m,p}$ ($[MeB(C_6F_5)_3]^-$) ≈ 5.0). For further details see Beringhelli, T.; Donghi, D.; Maggioni, D.; D'Alfonso, G. *Coord. Chem. Rev.* **2008,** *252*, 2292-2313.

(8) Dong, Z.; Reinhold, C. R.; Schmidtmann, M.; Müller, T. *J. Am. Chem. Soc.* **2017,** *139*, 7117-7123.

(9) Pyykkö, P.; Atsumi, M. *Chem. Eur. J.* **2009,** *15*, 12770-12779.

(10) Del Rio, N.; Lopez-Reyes, M.; Baceiredo, A.; Saffon-Merceron, N.; Lutters, D.; Müller, T.; Kato, T. *Angew. Chem. Int. Ed.* **2017,** *56*, 1365-1370.

(11) (a) Harlan, C. J.; Hascall, T.; Fujita, E.; Norton, J. R. *J. Am. Chem. Soc.* **1999,** *121*, 7274-7275. (b) Kwaan, R. J.; Harlan, C. J.; Norton, J. R. *Organometallics* **2001,** *20*, 3818-3820. (c) Beddows, C. J.; Burrows, A. D.; Connelly, N. G.; Green, M.; Lynam, J. M.; Paget, T. J. *Organometallics* **2001,** *20*, 231-233. (d) Ishida, Y.; Sekiguchi, A.; Kobayashi, K.; Nagase, S. *Organometallics* **2004,** *23*, 4891-4896. (e) Zheng, X.; Wang, X.; Qiu, Y.; Li, Y.; Zhou, C.; Sui, Y.; Li, Y.; Ma, J.; Wang, X. *J. Am. Chem. Soc.* **2013,** *135*, 14912-14915.

(12) Lawrence, E. J.; Oganesyan, V. S.; Wildgoose, G. G.; Ashley, A. E. *Dalton Trans.* **2013,** *42*, 782-789.

(13) Zanello, P. *Inorganic Electrochemistry: Theory, Practice and Application*; Royal Society of Chemistry: Cambridge, U.K., 2003.

(14) Connelly, N. G.; Geiger, W. E. *Chem. Rev.* **1996,** *96*, 877-910.

(15) Schäfer, A.; Reißmann, M.; Schäfer, A.; Saak, W.; Haase, D.; Müller, T. *Angew. Chem. Int. Ed.* **2011,** 50, 12636-12638.

(16) Mizuhata, Y.; Sasamori, T.; Tokitoh, N. *Chem. Rev.* **2009,** *109*, 3479-3511.

(17) Miller, J. S.; Min, K. S. *Angew. Chem. Int. Ed.* **2009,** *48*, 262-272.

Insert Table of Contents artwork here